AD-A105 968 BRIGHAM YOUNG UNIV PROVO UTAH DEPT OF CHEMICAL ENGI--ETC F/G 7/4
THE ELECTROCHEMISTRY OF MOLTEN LITHIUM CHLORATE AND ITS POSSIBL--ETC(U)
DEC 80 S S WANG, D N BENNION N00014-80-C-0345
UNCLASSIFIED BYU-TR-1 NL

1 OF 1
AD A
105 968

END
DATE FILMED
11-81
DTIC

LEVEL II

OFFICE OF NAVAL RESEARCH

Contract N0014-80-C-0345

Task No. NR 359-551

TECHNICAL REPORT NO. 1

The Electrochemistry of Molten Litnium Chlorate and its Possible Use with Litnium in a Battery

by

Su-Chee Simon Wang and Douglas N. Bennion

Brigham Young University

Department of Chemical Engineering

Provo, Utah 84602

Prepared for Publication

in the

Journal of The Electrochemical Society

(11) Dec[redacted]80

(12) 2

81 10 21

The Electrochemistry of Molten Lithium Chlorate and Its Possible Use With Lithium in a Battery

by

Su-Chee Simon Wang[1] and Douglas N. Bennion[2]

Chemical Engineering Department,

University of California, Los Angeles 90024

ABSTRACT

Lithium chlorate, $LiClO_3$, has a reported melting point of 127.6[5]°C or 129[4]°C. The specific conductance of molten lithium chlorate is relatively high compared to most electrolytic solutions used at room temperature. Therefore, lithium chlorate offers the chance to operate a new lithium battery system at a temperature between 130[4]°C and 150[6]°C. It is found from experiments that lithium chlorate is stable in the potential range between 3.2 V and 4.6 V relative to a Li reference electrode. A Li-Cl_2 secondary battery system has an open circuit potential of 3.97 V, making a Li-Cl_2 secondary battery in molten lithium chlorate, in principle, possible. A lithium-lithium chlorate primary battery system is also possible. Lithium negative electrode performance is hindered by corrosion and possible runaway reactions with $LiClO_3$ and dendrite formation on charging. The solubility of Li_2O and LiCl in $LiClO_3$ at 145[6]°C is ~~7.5 × 10⁻³~~ mol/cm³ and ~~1.18~~

x 10^{-3} mol/cm^3 respectively. The diffusion coefficients are 1.5 x 10^{-7} cm^2/s for Li_2O and 3.4 x 10^{-7} cm^2/s for LiCl. Platinum appeared to be an inert positive electrode for chlorate, chlorine, or oxygen reactions for short term runs, order of several hours. Nickel shows active-passive behavior which is complex. Nickel appears suitable for primary cell, cathodic discharge of $LiClO_3$, but it does not appear suitable for a Cl_2 or O_2 electrode.

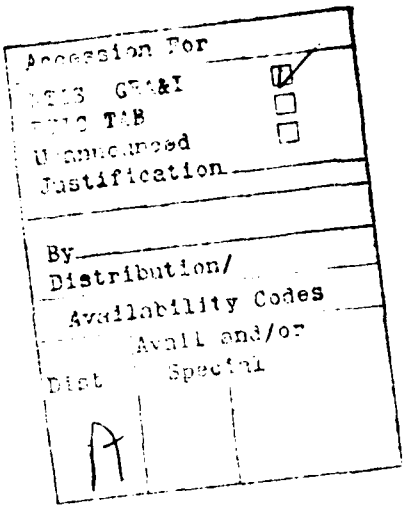

1) Present address: General Motors Research Laboratory, Warren, Mich., 48090.

2) Present address: Chemical Engineering Dept., Brigham Young University, Provo, Utah 84602.

Introduction

Lithium, with low equivalent weight and large negative electrochemical potential, is an attractive choice as a negative electrode for batteries of high specific energy and power density. Two types of nonaqueous lithium battery systems have been developed, ambient temperature and high temperature systems.

Compared to the ambient temperature systems, the high temperature systems have the advantage of higher power output capacity because of the higher conductivity and the faster electrode kinetics associated with molten salt electrolytes used in high temperature systems. However, disadvantages for high temperature systems are heated up in the starting up stage and the material problems of sealing and separation. Looking for a molten salt electrolyte which works at a lower temperature, e.g., below 200°C, might be one of the alternatives to solve the material problems.

Lithium chlorate, $LiClO_3$, has reported melting point about 128°C (1, 2). Therefore, lithium chlorate offers the chance to operate a new battery system at a temprature between 130° and 150°C. The specific conductance of molten lithium chlorate varies from 0.1150 $(ohm\ cm)^{-1}$ at 131.8°C to 0.1420 $(ohm\ cm)^{-1}$ at 143.01°C (3).

It is reported by Markowitz et al. (4) that after two days of heating at a temperature of 135°C under flowing argon, only 0.46% lithium chlorate was decomposed to either lithium chloride (0.06%) or lithium perchlorate (0.40%). It was also reported that the fast exothermic decomposition takes place at about 376°C. Lithium chlorate at about 140°C is believed to have good thermal stability.

In preliminary experiments, lithium could be successfully deposited and discharged reversibly on different inert negative electrode substrates including lithium, nickel, stainless steel, and platinum. All of these substrates are believed to be stable in molten lithium chlorate. However, the formation of a lithium-platinum alloy embrittled the platinum substrate.

The cathodic reaction occurring on the surface of an inert positive electrode during discharging is believed to be the reduction of lithium chlorate to lithium oxide and lithium chloride.

$$LiClO_3 + 6\ Li^+ + 6\ e^- \rightarrow LiCl + 3\ Li_2O \qquad (1)$$
$$E^\circ = 3.241\ V\ ^{(5,6)}\ \text{(relative to Li ref. electrode)}$$

The various anodic electrochemical reactions which are expected on the surface of a positive electrode during charging are

$$Li_2O \rightarrow 2\ Li^+ + \tfrac{1}{2}\ O_2 + 2\ e^- \qquad (2)$$
$$E^\circ = 2.903\ V\ ^{(6)}\ \text{(relative to Li ref. electrode)}$$
$$LiCl \rightarrow Li^+ + \tfrac{1}{2}\ Cl_2 + 2\ e^- \qquad (3)$$
$$E^\circ = 3.976\ V\ ^{(6)}\ \text{(relative to Li ref. electrode)}$$
$$LiClO_3 \rightarrow Li^+ + \tfrac{1}{2}\ Cl_2 + \tfrac{3}{2}\ O_2 + e^- \qquad (4)$$

$E^\circ = 4.6$ V (from experimental data, relative to Li ref. electrode)

In the present study, inert materials which can be used as positive or negative electrodes in molten lithium chlorate were studied. At different discharging states, the polarization experiments were conducted at various rotating disks, Ni and Pt, to study the effects of discharging products, presumably Li_2O and LiCl, on polarization curves. The electrolyte was also analyzed at different charging and discharging states to investigate the possible involvement of reactions (1), (2), (3), and (4) on inert positive electrodes. Gas, evolving from the positive electrode during charging, was collected and analyzed as a compliment to the information obtained from liquid phase chemical

analysis. The potential range, at which molten lithium chlorate is electrochemically stable, is discussed. The possibility of using lithium chlorate as the electrolyte in a primary and a secondary lithium battery is considered.

Experimental

Lithium chlorate used in all experiments was prepared as described by Campbell and Griffiths (7). A 1.0 M solution of barium chlorate was heated to 85°C. Then a 1.0 M solution of lithium sulfate was added slowly until equivalence was reached. The precipitated barium sulfate was removed by filtration. The lithium chlorate solution was evaporated slowly under 1 cm Hg pressure, the temperature being kept below 85°C, up to an approximate concentration of 90% lithium chlorate. The concentrated lithium chlorate solution was then transferred into an argon atmosphere glove box and heated to 130°C under 50 µm Hg pressure for four weeks. Using this process, the "dried" lithium chlorate melted between 126°C and 128°C. According to the chlorate-water phase diagram proposed by Krauss et al. (8), the melting point of lithium chlorate between 126°C and 128°C corresponds to a water content of less than 0.5%. Lithium chlorate is known to be extremely hygroscopic (8). Although the water content in lithium chlorate was 0.5% or less, no gross effects associated with water were observed. The 50 µm of Hg pressure in the drying chamber was mostly argon leaking into the flask. Thus, the partial pressure of water was some small fraction of 50 µm of Hg at 130°C.

The polarization experiments were conducted in rotating disk cells. The rotating disk cell was composed of a glass cylinder 3/4 inch in diameter and 1 and 1/2 inch high, to accommodate both the rotating disk and molten lithium chlorate. Two glass tubes, 0.6 cm in diameter, were connected to the cylinder at the bottom accommodating a lithium counter electrode in one tube and a lithium reference electrode in the other. Small sintered glass blocks 1/8 inch thick were embedded

inside the 0.6 cm tubes to separate the main cylinder from the lithium counter electrode and the reference electrode. Nickel and platinum rotating disks were employed. The nickel rotating disk was made of a nickel rod, 1/8 inch in diameter and 1 and 7/8" long, held inside a teflon sleeve 0.3 inch in diameter. The platinum rotating disk was made of a platinum wire, 0.051 inch in diameter, surrounded by a 0.3 inch diameter teflon sleeve and supported by an aluminum rod, 1/8 inch in diameter.

The rotating disk cell was placed on a hot plate surrounded by a heavy aluminum tube, 1/4 inch wall thickness, forming a cavity which is at a reasonably constant temperature, $\pm$ 1°C. Temperature was measured using an iron-constantan thermocouple. The temperature was kept at 145°C during experimental runs. About 6.5 grams of pure lithium chlorate was added into the main cylinder. The two side arms were half filled. Two lithium ribbons, one inserted into the counter electrode compartment and the other inserted into the reference electrode compartment, were held in position by two teflon stoppers. Then the rotating disk electrode was dipped into the molten lithium chlorate contained in the main cylinder. The rotating speed, controlled by an adjustable motor, was generally kept at 1000 rpm, but sometimes varied between 1000 and 1300 rpm.

All experiments were performed in an argon filled glove box, Model HE-243-2 DRI LAB, which was supplied by Vacuum Atmosphere Corporation. The impurity levels of oxygen and water can be estimated by measuring the life of a 25 watt light bulb tungsten filament in the glove box. The light burned for a month, indicating, according to the operating manual of the dri-lab, that the oxygen plus water content was between

1 and 5 ppm. The temperature within the glove box was kept at 29 $\pm$ 1°C.

The circuit is composed of a potentiostat and an ammeter for measuring the current, connected in series with the experimental cell. A digital voltmeter was connected between the rotating disk electrode and the lithium reference electrode for measuring the potential. All of the polarization curves were obtained potentiostatically.

The chemical analysis for chloride ions and oxide ions suggested by Markowitz (5) was employed to investigate the involvement of lithium chloride and lithium oxide in the electrochemical reaction, occurring on the positive electrode of a lithium chlorate cell. After charging and discharging at various potential plateaus observed in the polarization experiments, lithium chlorate electrolyte was sampled and dissolved in distilled water. The oxide content was determined by titration to the phenophthalein end point with hydrochloric acid; chloride content was determined gravimetrically as AgCl. The Ni content in the electrolyte was measured using a Perkin-Elmer Atomic Absorption Spectrometer.

Gas, often observed evolving from the positive electrode during charging, was collected and analyzed as a complement to the information obtained from liquid phase chemical analysis.

Results

In the first polarization experiments, 6.3085 grams of fresh lithium chlorate were added into the main cylinder of a rotating disk cell. A Ni rotating disk, polished before using, was then dipped into molten lithium chlorate electrolyte and left standing hot until the open circuit potential reached a steady state. In Figure 1, the anodic polarization curve in fresh lithium chlorate is shown. Discharging or cathodic reaction of the lithium chlorate was conducted afterwards employing a Ni plate 1 cm x 1 cm area in the main cylinder and running current between the Ni plate and the Li counter electrode. At different discharging stages of the electrolyte, after 200, 600, 1000 micro equivalents discharged, anodic polarization curves were obtained on a freshly polished Ni rotating disk. These curves are shown in Figure 2. After 1500 micro equivalents discharged from the lithium chlorate, three anodic polarization curves were run on a Ni rotating disk, the first one right after discharging, the second two hours after discharging, and the third twenty hours after discharging. The disk was polished before the first run and left standing in molten lithium chlorate afterwards. These three curves are shown in Figure 3.

Comparing Figure 1, 2, and 3 shows that the first plateau, 3.0 V, appeared in Figure 2 after 1000 micro equivalents discharged. However, this plateau was partially or completely eliminated in Figure 3 after the Ni rotating disk was left standing hot in molten lithium chlorate for two or twenty hours, respectively. It was also observed that the second plateau, 3.6 V in Figure 1 or 3.3 V in Figure 2 and 3, extends further after discharging. The 4.7 V plateau or the third plateau appeared at a lower potential when fresh lithium chlorate

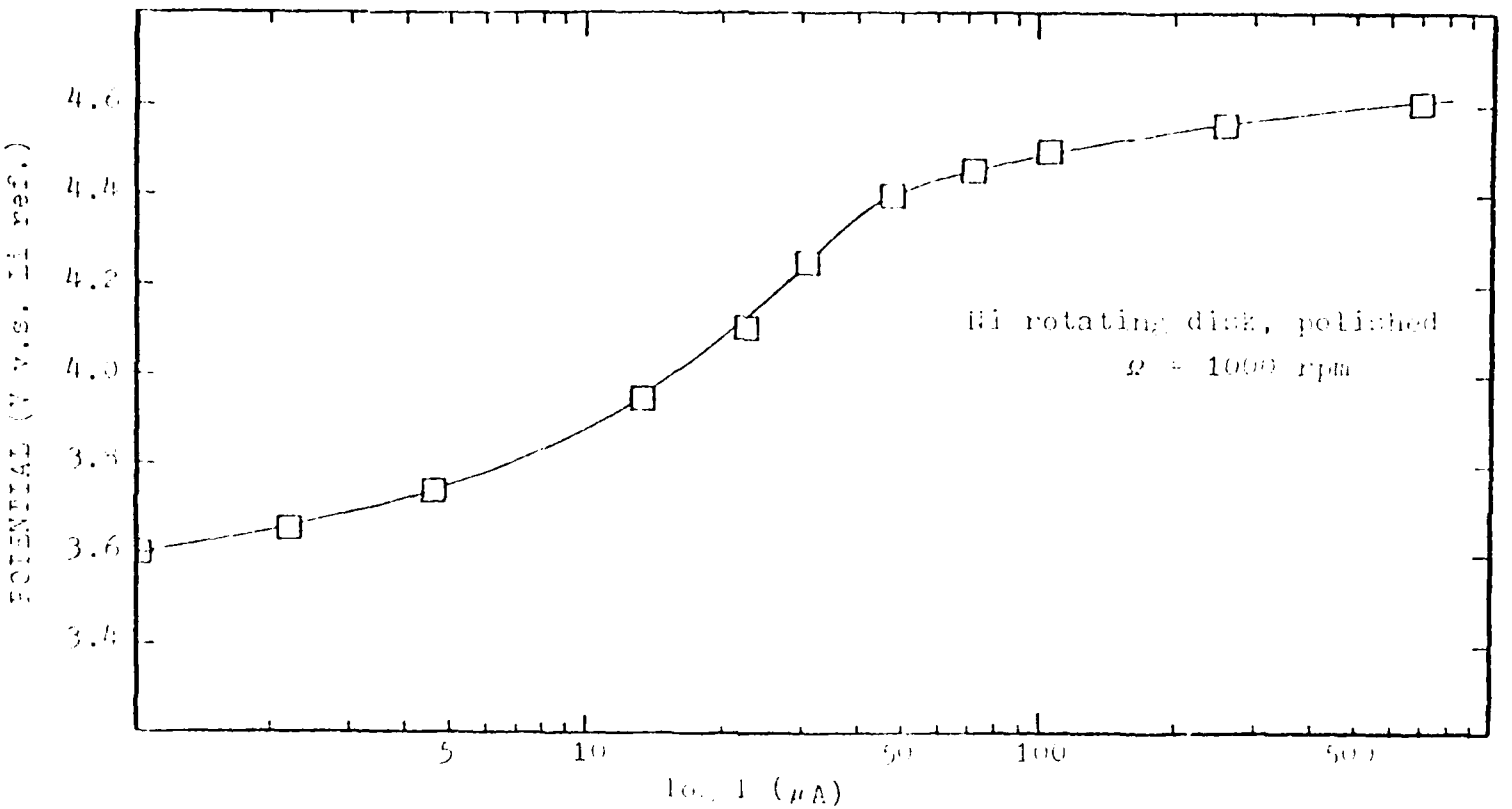

Figure 1. Anodic polarization curve in fresh lithium chlorate

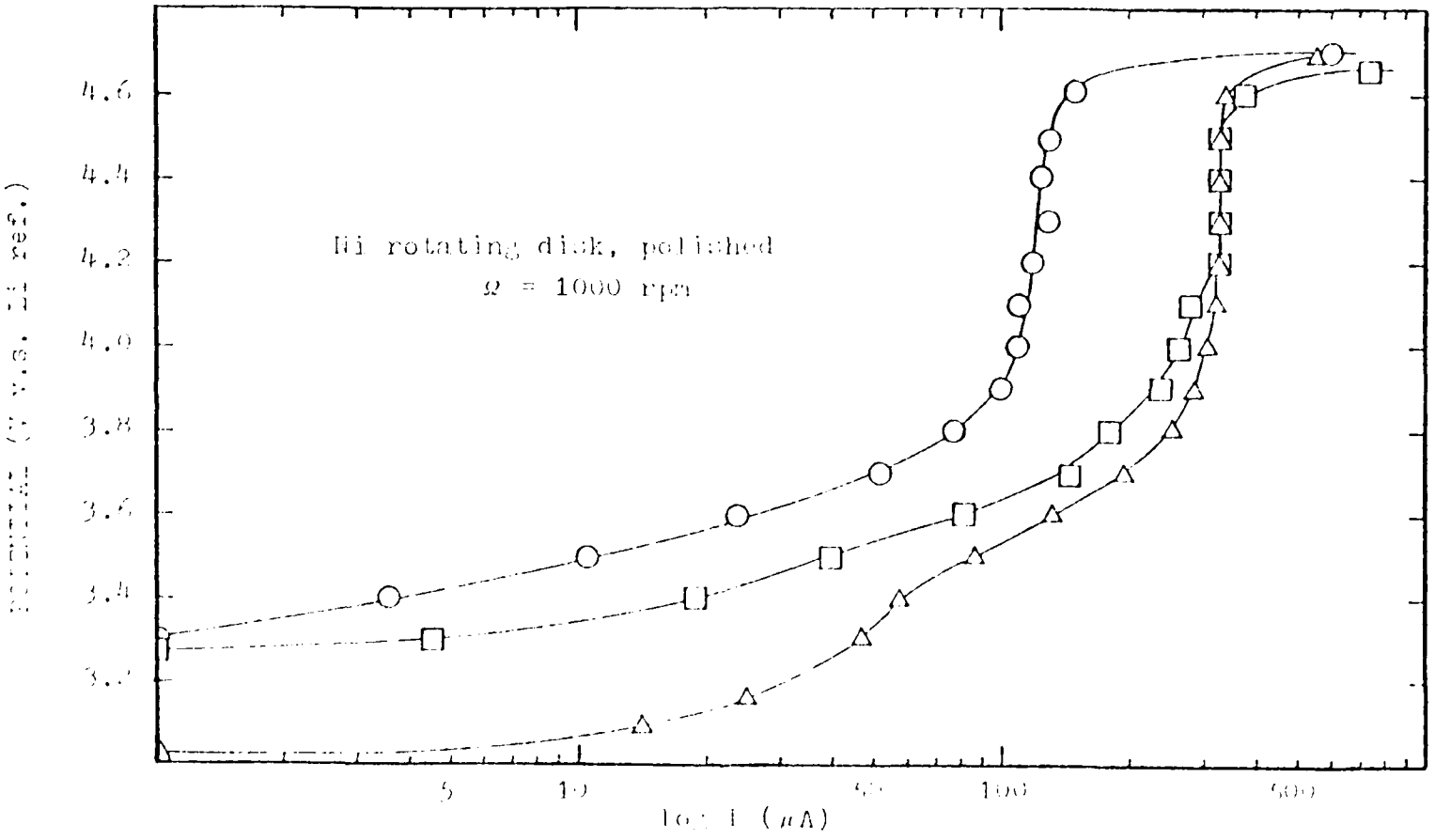

Figure 2. Anodic polarization curves at different discharging stages, after ○200 micro equivalents, □600 micro equivalents, △1000 micro equivalents discharged.

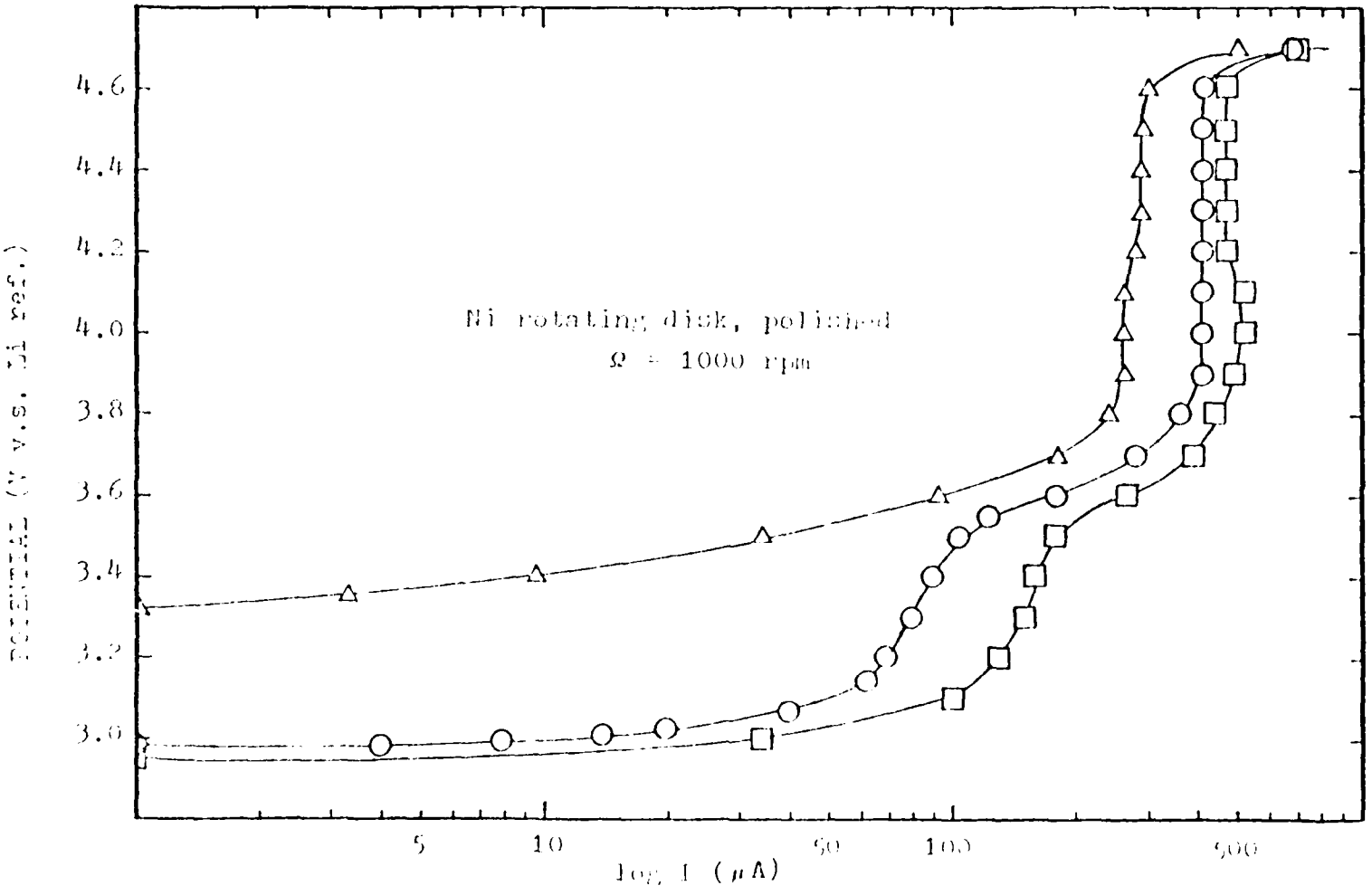

Figure 3. Anodic polarization curves after 1500 micro equivalents discharged □right after discharging, ○after two hours hot stand, and Δ after 20 hours hot stand.

was used as the electrolyte.

In the second set of experiments, 6.448 grams of fresh lithium chlorate was added into the main cylinder of a rotating disk cell. After 400 micro equivalents was discharged from the electrolyte using a Ni plate 1 cm x 1 cm area, anodic polarization experiments were run on a polished Ni rotating disk at different rotating speeds. In Figure 4, anodic polarization data, with ω = 1000 rpm, 1200 rpm, 1500 rpm, and 1800 rpm, are shown. It was found that the limiting current observed between the second and the third plateaus obeyed the square root law, i.e., $I_L \propto \sqrt{\omega}$, of Levich's Equation (9).

$$I_L = 0.62nFAD_o^{2/3}\nu^{-1/6}\omega^{1/2}C_o \qquad (5)$$

The lithium chlorate electrolyte was then further discharged using the Ni plate. At various discharging stages of the electrolyte, 530, 630, and 704 micro equivalents discharged, anodic polarization curves were taken on a polisned Ni rotating disk. The limiting current observed on anodic polarization curves, shown in Figure 5, reached a constant value of 290 mA after 630 micro equivalents discharged.

Cathodic polarization curves were also taken in the electrolyte after 704 micro equivalents discharged. The curves, shown in Figure 6, indicated that the cathodic current could be enhanced at a higher rotating speed but the square root law did not hold here.

In the following described experiments, a polished Pt rotating disk was dipped into 6.912 grams of fresh lithium chlorate. The anodic polarization curve was taken in the fresh electrolyte as shown in Figure 7. After 250 and 450 micro equivalents discharged from the electrolyte using a Ni plate, anodic polarization experiments were run on a polished Pt rotating disk at two different rotating speeds,

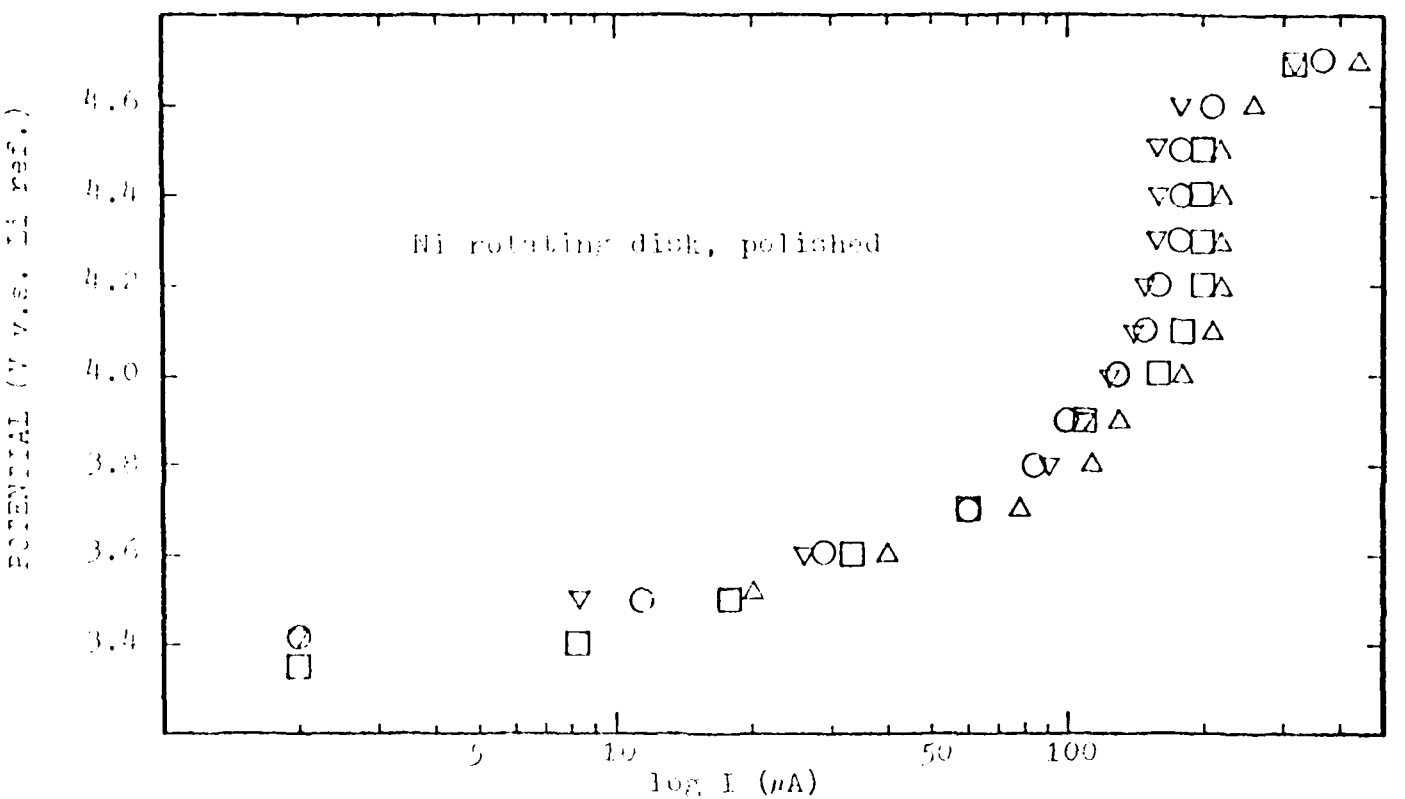

Figure 4. Anodic polarization curves after 400 micro equivalents discharged ▽ ω = 1000 rpm, ○ ω = 1200 rpm, □ ω = 1500 rpm, and △ ω = 1800 rpm.

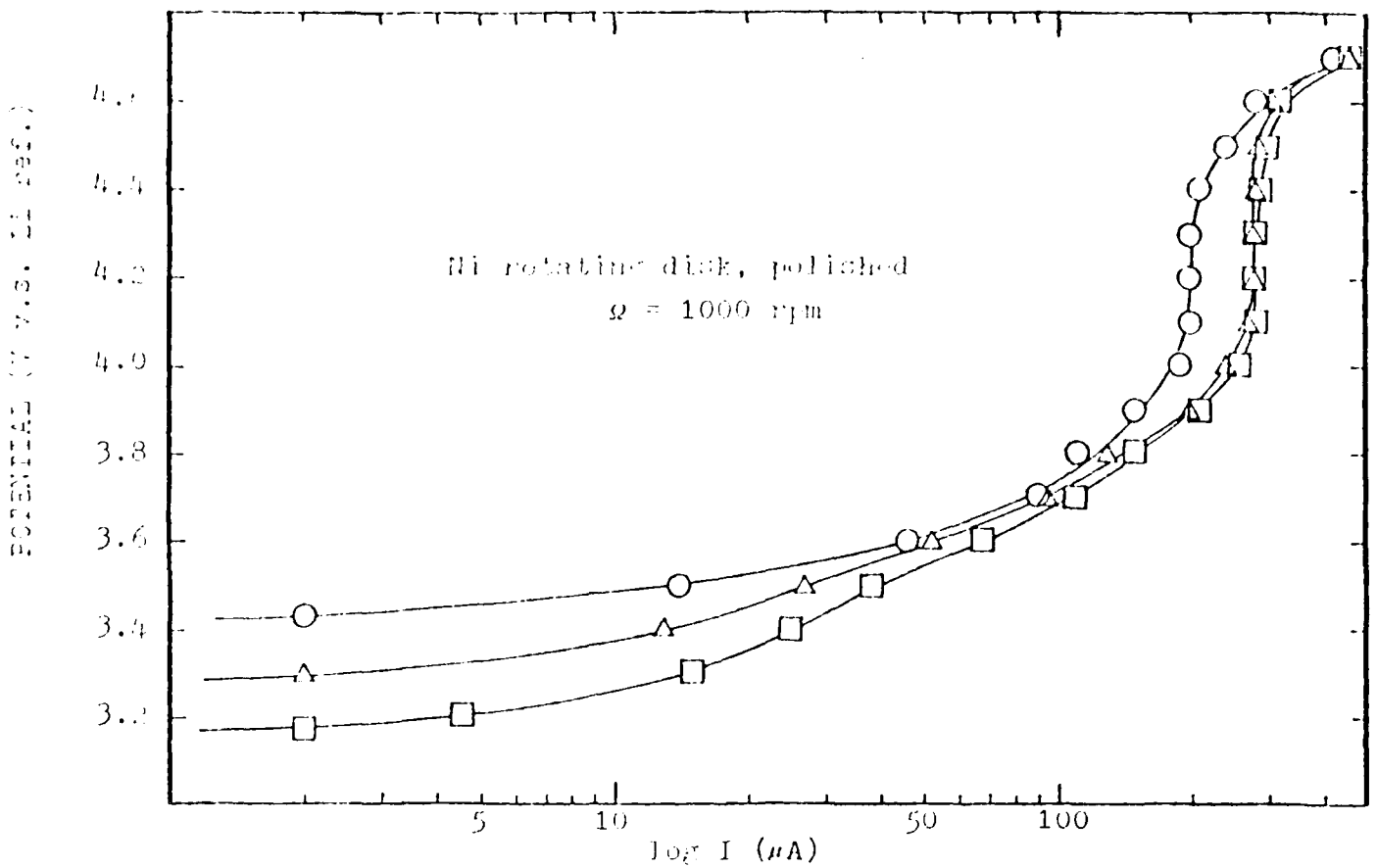

Figure 5. Anodic polarization curves at different discharging stages, after ○530 micro equivalents, □630 micro equivalents, △704 micro equivalents discharged.

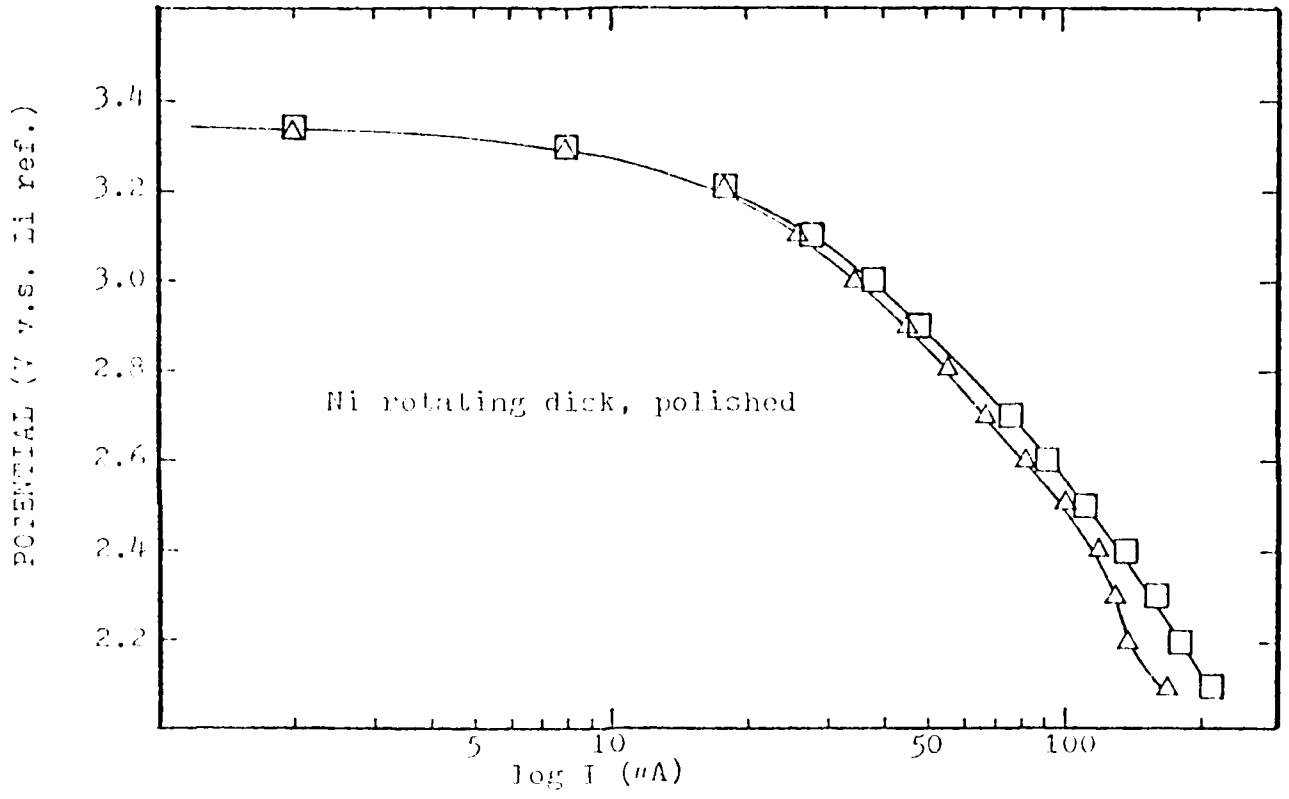

Figure 6. Cathodic polarization curves after 704 micro equivalents discharged, △ Ω= 1000 rpm, □ Ω= 1500 rpm.

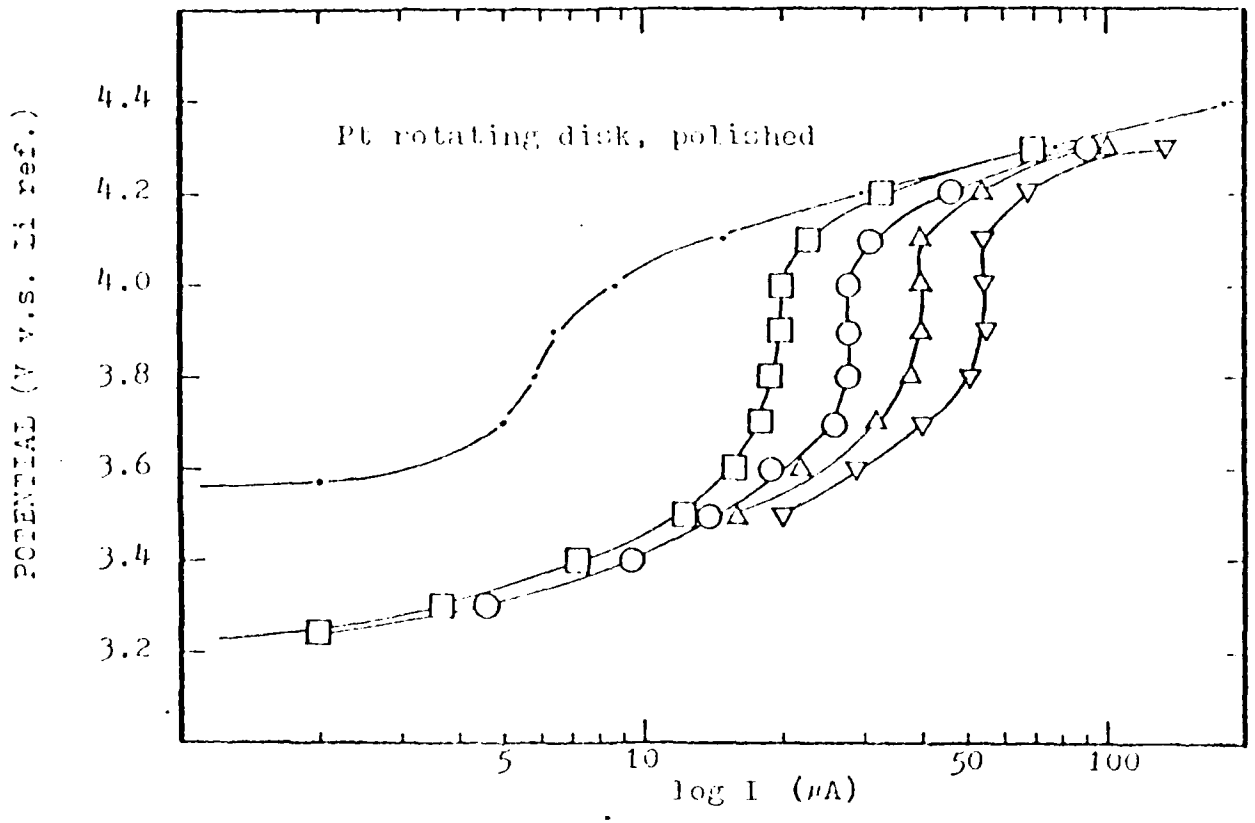

Figure 7. Anodic polarization curves, • in fresh lithium chlorate Ω = 1000 rpm, □ after 250 micro equivalents discharged Ω = 1000 rpm, ○ after 250 micro equivalents discharged Ω = 1300 rpm, △ after 450 micro equivalents discharged Ω = 1000 rpm, ▽ after 450 micro equivalents discharged Ω = 1300 rpm.

1000 rpm and 1800 rpm. The limiting current between 3.2 V and 4.2 V plateaus for the anodic polarization curves followed the square root law.

Cathodic polarization curves on Pt in either fresh lithium chlorate or after 450 micro equivalents discharged are shown in Figure 8 and 9 for 1000 rpm and 1800 rpm. The cathodic current increased at higher rotating speed but less than $\sqrt{\omega_1/\omega_2}$, similar to cathodic current on a Ni rotating disk. The cathodic limiting current decreased with an increase in the extent of discharging.

The plateau, appearing between 4.0 and 4.6 V of the anodic polarization curves on Pt rotating disks, was studied further in the following experiments. Vacuum dried LiCl was added into 8.32 grams of molten lithium chlorate step by step; therefore, anodic polarization curves at different LiCl concentration could be obtained on a polished Pt rotating disk. At an analyzed LiCl concentration of 1.542×10^{-3} mole/ cm^3, polarization experiments were conducted at two different rotating speeds, 1000 and 1800 rpm. Two limiting currents, 90 μA and 120 μA respectively, were observed as shown in Figure 10. At higher concentration, 1.574×10^{-3} mole/cm^3, the limiting current increased to 820 μA at a rotating speed of 1000 rpm. When the lithium chlorate was saturated with LiCl, the limiting current increased to 1000 μA at 1000 rpm. A new plateau above 4.6 V is observed in all cases.

The involvement of Li_2O and LiCl in the electrochemical reactions on the positive electrode in a lithium chlorate was explored further by chemical analysis for LiCl and Li_2O [5,]. The lithium chlorate electrolyte was sampled periodically from the positive compartment

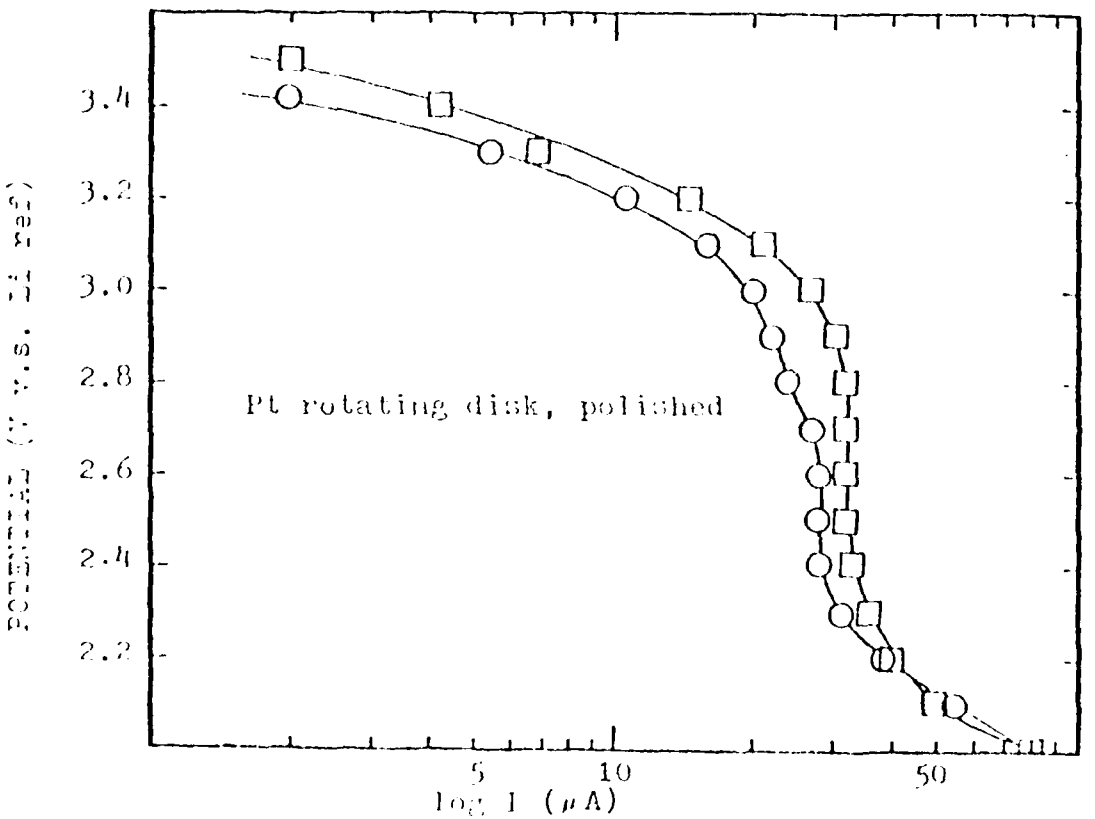

Figure 8. Cathodic Polarization curves in fresh lithium chlorate, ○ Ω = 1000 rpm, □ Ω = 1800 rpm.

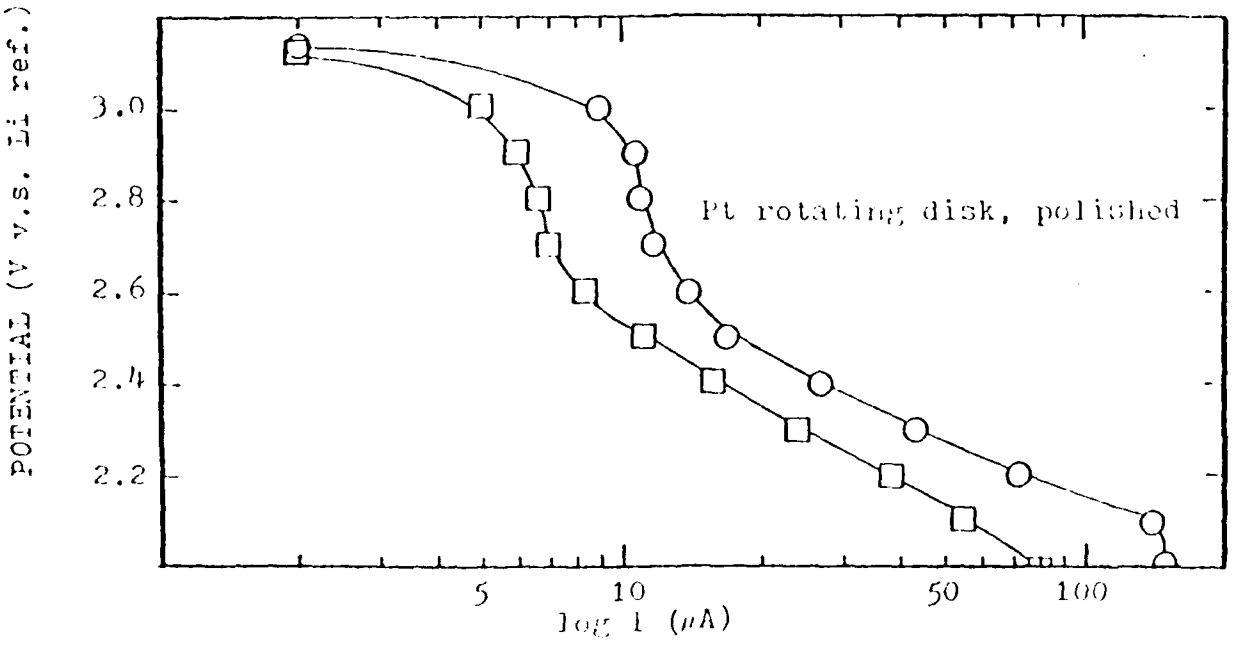

Figure 9. Cathodic polarization curves after 450 micro equivalents discharged, □ Ω = 1000 rpm, ○ Ω = 1800 rpm.

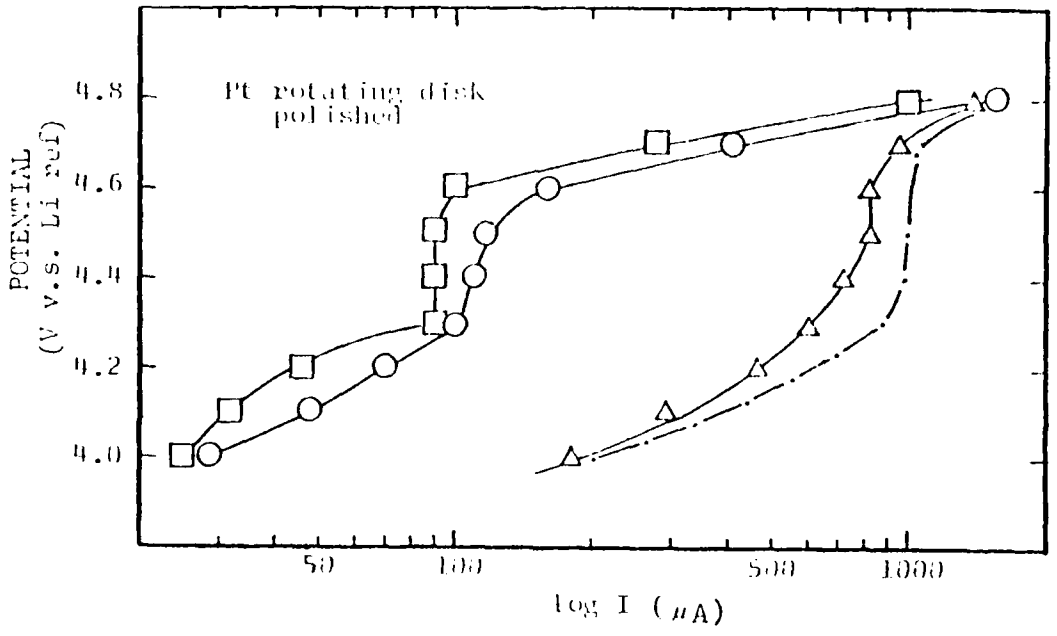

Figure 10. Anodic polarization curves at different LiCl concentration,
□ c = 1.542×10^{-4} mol/cm³ Ω = 1000 rpm, ○ Ω= 1800 rpm
△ c = 1.574×10^{-3} mol/cm³ Ω = 1000 rpm,
• saturated with LiCl Ω = 1000 rpm.

during discharging around 2.5 V using a Ni or a Pt positive electrode. The sampled electrolyte was then analyzed. The results are summarized in Table 1. It was found that about 20% less Li_2O and 30% more LiCl than expected based on Equation (1) were created during discharging of the electrolyte.

After discharging around 2.5 V, charging was conducted in the electrolyte using a Ni or a Pt electrode. Charging current was adjusted occasionally to keep the potential between 3.0 and 3.8 V. The electrolyte was sampled from the positive compartment after charging and analyzed for Li_2O and LiCl. It was found that only Li_2O was consumed during charging, see Table 2.

Gassing has been observed during charging between 3.0 V and 3.8 V on either Ni or Pt electrodes. The gas, collected from the positive compartment, was blown through oxygen absorbent to analyze the oxygen content. The results are shown in Table 3. Based on the results shown in Table 2 and 3, it is believed that the electrochemical reaction occurring on the positive electrode during charging between 3.0 V and 3.8 V is oxygen evolution from Li_2O, Equation (2).

When charging was carried out between 4.4 V and 4.7 V on a Ni positive electrode, the electrolytic solution became dark green in color. The chemical analysis of the electrolyte showed that Li_2O and LiCl were neither created nor consumed. However, after dissolving the electrolyte and the dark green precipitate in acid, nickel ions were found quantitatively in the solution using an atomic absorption spectrometer.

When charging was carried out between 4.0 V and 4.6 V on a Pt positive electrode, it was found that both LiCl and Li_2O were consumed,

Table 1

Summarized Results of Chemical Analysis
After Discharging Using a Ni or a Pt Electrode

Type of Electrode	Ni	Ni	Pt
Amount of $LiClO_3$ in the positive compartment	5.0051 g	4.6385 g	5.3085
Amount of discharge	1200 micro equivalent	2200 micro equivalents	600 micro equivalents
Amount of Li_2O created during discharging	476.93 micro moles (953.86 micro equivalents)*	921.55 micro moles (1843.10 micro equivalents)*	242.33 micro mole (484.76 micro equivalents)*
Amount of LiCl created during discharging	264.45 micro moles (1886.70 micro equivalents)*	500.45 micro moles (3002.70 micro equivalents)*	128.9 micro mole (773.4 micro equivalents)*

*converted based on Equation (1)

Table 2

Summarized Results of Chemical Analysis
After Charging Using a Ni or a Pt Electrode below 3.8V

Type of Electrode	Ni	Pt
Amount of $LiClO_3$ in the positive compartment	4.6005 g	5.1933 g
Amount of charge	500 micro equivalent	437.15 micro equivalent
Amount of Li_2O consumed during charging	203.7 micro moles (407.4 micro equivalents)*	173.81 micro moles (347.62 micro equivalents)*
Amount of LiCl consumed during charging	—	—

* calculated based on Equation (2)

Table 3

The results of oxygen collection
during charging between 3.0 and 3.8V

Testing electrode	Amount of charge (micro equivalents)	Amount of gas collected (ml)	Oxygen content in the collected gas (ml)
Ni	200	1.6	1.2 (195 micro equivalent) *
Pt	200	1.6	1.1 (179 micro equivalents) *

* converted based on Equation (2)

Table 4

Summarized Results of Chemical Results After
Charging above 4.0 V Using a Pt Positive Electrode

Amount of $LiClO_3$ in the positive electrode	4.921 g	5.468 g
Amount of Charge	600 micro equivalents	600 micro equivalents
Charging potential	4.0 to 4.6 V	above 4.6 V
Amount of Li_2O consumed during charging	196.1 micro moles	164.9 micro moles
Amount of LiCl created or consumed during charging	90.57 micro mole consumed	80.11 micro moles created

Table 5

The Results of Gas Collection on Pt Electrode
during Charging above 4.0V

No. of Charging	Amount of Charge (micro equivalents)	Charging Potential (V)	Charging Current (mA)	Amount of Cl_2 evolved (micro equivalents)*	Amount of Oxygen evolved (ml)
1	150	4.72	15	111.48	3.20
2	150	4.72	15	131.56	3.80
3	150	4.72	15	132.57	3.60

*converted based on Equation (4)

see Table 4. However, during charging above 4.6 V, LiCl is created as Li_2O is consumed on a Pt positive electrode.

During charging above 4.6 V on a Pt positive electrode, gas was collected and analyzed for both Cl_2 and O_2. From the results shown in Table 5, it was observed that Cl_2 was evolved quantitatively along with a certain quantity of oxygen during anodic charging above 4.6 V.

Discussion

From Table 1, it is proved that the cathodic reaction occurring on a positive electrode, Ni or Pt, during discharging is the reduction of $LiClO_3$ to form Li_2O and LiCl, Equation (1).

$$LiClO_3 + 6\ Li^+ + 6\ e^- \rightarrow LiCl + 3\ Li_2O \qquad (1)$$

The reason that less Li_2O is shown created in Table then theoretically predicted from Faraday's law applied to Equation (1) might be associated with the migration of oxide ions through the sintered glass separator and into the negative compartment. In the meantime, more LiCl is found than expected from Faraday's law applied to the single reaction of Equation (1). The decomposition reaction of $LiClO_3$ to LiCl and O_2 besides the reaction of Equation (1) takes place on a positive electrode accounting for the extra LiCl, since 2.5 cc of oxygen has been collected during 1125 micro equivalents discharged.

During charging between 3.0 and 3.8 V, oxygen evolution from Li_2O occurs on a Ni or Pt positive electrode, see Table 3.

$$Li_2O \rightarrow 2\ Li^+ + \tfrac{1}{2}\ O_2 + 2\ e^- \qquad (2)$$

The transition between the second and the third plateau in anodic polarization curves is due to the mass transfer control of Li_2O to the rotating disk, since the limiting current increases with increase in concentration of Li_2O. The diffusion coefficient in molten lithium chlorate can be estimated using Levich's equation (9).

$$I_L = 0.62\ n\ F\ A\ D^{2/3}\nu^{-1/6}\Omega^{1/2}C \qquad (5)$$

where I_L, the limiting current; F, the Faraday constant; A, the disk area; D, the diffusion coefficient of Li_2O; ν, the kinematic viscosity of the electrolyte; Ω, the angular velocity of the disk; and C, the concentration of Li_2O. The n is equal to 2 in this case since two

electrons are given up by each Li_2O molecule during charging. The ν can be calculated using the equation suggested by Campbell et al. (10) for pure lithium chlorate.

$$\nu(cm^2/sec) = \frac{1.979 \times 10^{-5}}{\rho} \cdot e^{7813/RT} \qquad (6)$$

T between 128° and 170°C
R = 1.987 cal/g-mol·°K

The densities of lithium chlorate, ρ, at various temperature, are also reported by Campbell et al. (11). Accordingly, the diffusion coefficient of Li_2O in lithium chlorate at 145°C is evaluated from Figure 7 with ν is equal to 0.116 cm^2/sec. The diffusion coefficient of Li_2O at various limiting current and measured Li_2O concentration are shown below.

$D = 1.40 \times 10^{-7}$ cm^2/sec as $I_L = 20$ μA $C_{Li_2O} = 3.221 \times 10^{-5}$ mole/cm^3
$D = 1.49 \times 10^{-7}$ cm^2/sec as $I_L = 28$ μA $C_{Li_2O} = 3.221 \times 10^{-5}$ mole/cm^3
$D = 1.50 \times 10^{-7}$ cm^2/sec as $I_L = 40$ μA $C_{Li_2O} = 6.135 \times 10^{-5}$ mole/cm^3
$D = 1.52 \times 10^{-7}$ cm^2/sec as $I_L = 54$ μA $C_{Li_2O} = 6.135 \times 10^{-5}$ mole/cm^3

The small value of these diffusion coefficients is due to the high viscosity of molten salt compared to aqueous solution, since diffusion coefficients times viscosity is a constant i.e. Walton's rule. These four diffusion coefficient deviate less than 8% from each other implying that the Li_2O is indeed the diffusion limiting species.

In Figure 5, it is shown that the limiting current reaches a constant value of 290 μA, after 630 micro equivalents were discharged. It is believed that this constant value is associated with the saturated concentration of Li_2O in lithium chlorate. Therefore, the solubility of Li_2O in lithium chlorate can be evaluated from Equation (5) to be 7.5×10^{-5} mole/cm^3 using the average diffusion coefficient of Li_2O, i.e., 1.48×10^{-7} cm^2/sec.

In Figure 10, it was observed that the length of the plateau between 4.0 and 4.6 V on Pt rotating disks is proportional to the concentration of LiCl in electrolyte. Therefore, it is believed that chlorine evolution from LiCl takes place on Pt electrodes during charging between 4.0 and 4.6 V.

$$LiCl \rightarrow Li^+ + \tfrac{1}{2} Cl_2 + e^- \quad (3)$$
$$E^\circ = 3.976V \quad (6) \quad \text{(relative to Li ref. electrode)}$$

The limiting current, observed in Figure 10, is apparently due to the mass transfer limitation of LiCl to Pt rotating disks. Accordingly, the diffusion coefficient of LiCl in the electrolyte could be estimated from Equation (5). At different LiCl concentration and limiting current, the diffusion coefficients are listed below.

$D = 3.60 \times 10^{-7}$ cm^2/sec as I_L = 90 μA $C_{LiCl} = 1.542 \times 10^{-3}$ mole/cm^3
$D = 3.56 \times 10^{-7}$ cm^2/sec as I_L = 110 μA $C_{LiCl} = 1.542 \times 10^{-3}$ mole/cm^3
$D = 3.04 \times 10^{-7}$ cm^2/sec as I_L = 820 μA $C_{LiCl} = 1.574 \times 10^{-3}$ mole/cm^3

The small value of these diffusion coefficients is again due to the high viscosity of molten salt compared to aqueous solution. The aggreement between these results with a standard deviation of 0.255 supports the conclusion that LiCl is the limiting diffusion reactant for the third charging plateau.

The solubility of LiCl in lithium chlorate can be estimated using the limiting current shown in Figure 10. When the electrolyte was saturated, a limiting current of 1000 μA was observed. Using the average diffusion coefficient of LiCl in lithium chlorate, the solubility of LiCl in lithium chlorate is 1.78×10^{-3} mole/cm^3 at 145°C. In Table 4, it shows that Li_2O was also consumed during charging between 4.0 and 4.6 V at the Pt electrode. This could be interpreted as follows. Since the charging potential employed is higher than oxygen evolution potential, the oxygen evolution occurring at about

3.4 V must be running at its limiting current during the entire charging. In addition, the replacement reaction between Li_2O and Cl_2 consumes Li_2O to reform LiCl.

$$Li_2O + Cl_2 \rightarrow 2\ LiCl + \tfrac{1}{2}\ O_2 \qquad (7)$$

$$\Delta G = -49.5\ \text{Kcal/mole} \qquad (6)$$

This also explains why in Table 4 less LiCl was consumed than expected based on Faraday's law.

In Table 5, the results show that oxygen along with chlorine is evolved from the Pt electrode during charging above 4.6 V. For instance, 3.80 cc or 150 micro mole (600 micro equivalents) of oxygen was collected in run number 2 while 150 micro equivalents was charged in at 4.72 V. If oxygen is evolved from Li_2O, that much O_2 is not expected. Therefore, it is believed that both chlorine and oxygen are evolved from lithium chlorate during charging above 4.6 V.

$$LiClO_3 \longrightarrow Li^+ + \tfrac{1}{2}\ Cl_2 + \tfrac{3}{2}\ O_2 + e^- \qquad (4)$$

Part of the chlorine gas evolved will react with Li_2O to form LiCl and O_2. This replacement reaction, Equation (7), lowers the concentration of Li_2O and creates LiCl. Since chlorine evolution from LiCl is also occurring at its limiting current when charging above 4.6 V, LiCl is created and consumed simultaneously by different reactions during charging. This explains why only 80 micro moles of LiCl were created while 165 micro moles of Li_2O were consumed (Table 4).

Chlorine evolution is not observed on Ni although a charging plateau around 4.6 V for a Ni rotating disk appears. From chemical analysis, it is found that Ni is oxidized to NiO during charging above 4.6 V.

The first charging plateau, observed on a Ni rotating disk in Figure 3, appears at a potential close to the standard potential

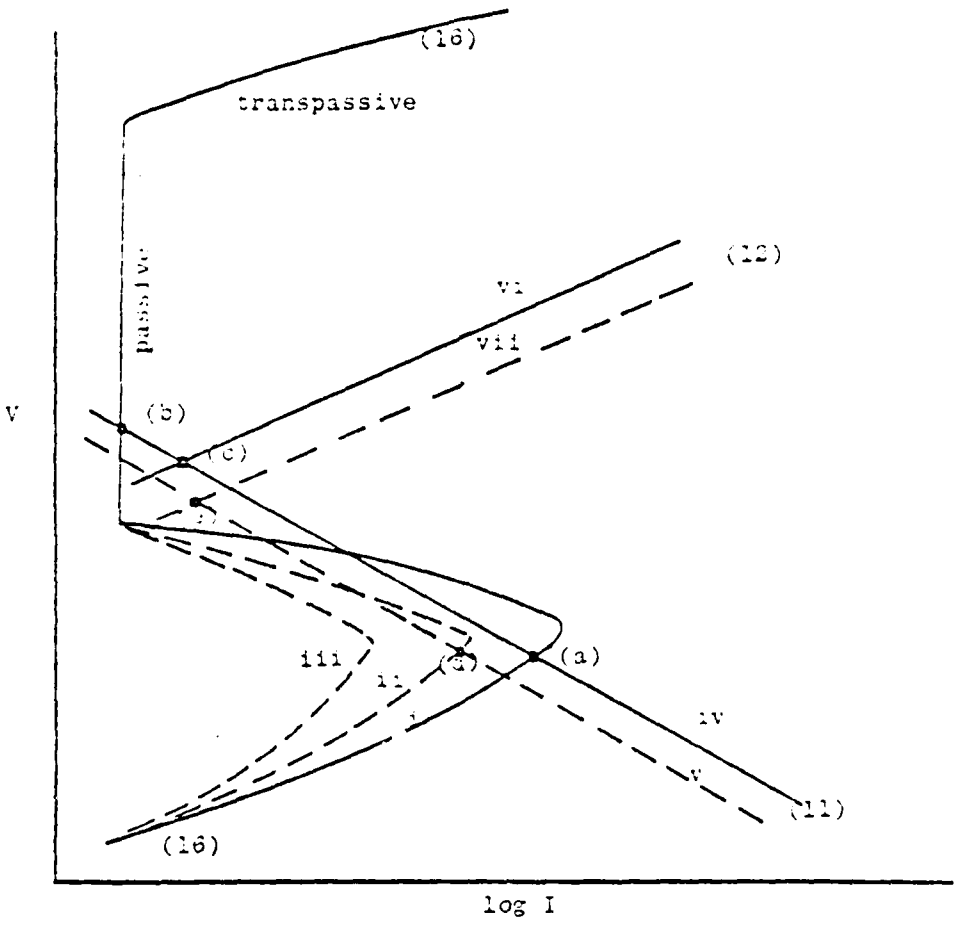

(11) $LiClO_3 + 6Li^+ + 6e^- \longrightarrow LiCl + 3Li_2O$

(12) $Li_2O \longrightarrow 2Li^+ + \frac{1}{2}O_2 + 2e^-$

(16) $Ni \longrightarrow Ni^{+2} + 2e^-$

Figure 11. The change of mixed potential of Ni in Molten Lithium Chlorate.

of the Ni electrode.

$$Ni \rightleftharpoons Ni^{+2} + 2\,e^-_{(2)} \qquad (3)$$
$$E^\circ = 2.799V \text{ (relative to Li ref. electrode)}$$

Therefore, it is believed that the first charging plateau is due to Ni dissolution and the third plateau is probably in the transpassive region. The mechanism of Ni passivation is described as follows.

As a polished Ni electrode is dipped into fresh molten lithium chlorate, a thin NiO film is believed to form on the surface of the Ni. This film could reduce the active area for Ni dissolution and shift Ni dissolution curve i to ii as shown in Figure 11. Then the mixed potential would be switched from (a), in Figure 11, to (b) or (c). The points (b) and (c) are the intersections of curve (iv) for lithium chlorate reduction with curve ii for Ni dissolution and curve vi for oxygen evolution, respectively. A mixed potential at point (b) or (c) implies that Ni is passivated and the first charge plateau for nickel dissolution is no longer seen on the Ni rotating disk, (see Figure 1).

Lithium oxide and lithium chloride are formed in the molten litnium chlorate during discharge using Ni plates. As discharge goes on, Li_2O will start to precipitate on the electrode after the electrolyte is saturated with Li_2O. This Li_2O precipitate could reduce the active area for litnium chlorate reduction and move curve iv gradually toward curve v. Finally, the cathodic curve v for lithium chlorate reduction will intersect the Ni dissolution curve ii in its active region, namely, point (d) in Figure 11, and reactivate nickel dissolution.

When the nickel is reactivated, the first charging plateau appears again. As shown in Figure 2, after 1000 micro equivalents discharged from lithium chlorate, the first charging plateau was observed

for a rotating disk.

The reactivated Ni is then reacting with molten lithium chlorate to form a more complete nickel oxide protective film. Eventually, the Ni will be passivated again, and the Ni dissolution curve is shifted to iii in Figure 11. Since more Li_2O is present in the electrolyte after discharging the lithium chlorate, the oxygen evolution curve is also shifted from vi to vii. Therefore, the mixed potention switches to the intersection of curve ii and vii, i.e. point (e) in Figure 11. This could explain the disappearance of the first charging plateau after hot stand, see Figure 3.

Pure lithium works to some extent as a Li negative electrode. The dendrite problem occurring on a pure Li negative electrode is serious. It might be solved using a lithium alloy such as Li-Al (12). The corrosion reaction between Li and molten lithium chlorate is estimated to be higher than $0.3mA/cm^2$ as Li_2O and LiCl are formed. No way to control this corrosion while the $LiClO_3$ is molten is now known. Therefore, if lithium chlorate is to be used as electrolyte in a lithium battery system, room temperature storage as a solid will be necessary to limit the corrosion reaction. The calorimetric data on lithium chlorate, given by Campbell et al. (10), suggests that 5491 cal/mole is needed for one mole of lithium chlorate to raise the temperature from 25^{o} to $145^{o}C$.

Conclusion

Based on the experimental results, it is known that lithium chlorate is stable in the potential range between 3.2 V and 4.6 V. Above 4.6 V, lithium chlorate will degrade to O_2, Cl_2, and Li^+ during charging. Below 3.2 V, lithium chlorate will reduce to LiCl and Li_2O.

Therefore, lithium chlorate can be used as the inert electrolyte of a lithium secondary battery only if the operating potential is between 3.2 V and 4.6 V. The Cl^-/Cl_2 half cell operates in this potential region on platinum.

A Li-$LiClO_3$ primary battery system is possible. With an energy density of 3898 Wh/kg based on a discharge potential of 3.2 V, the lithium chlorate primary battery is theoretically one of the highest specific energy primary batteries available.

Acknowledgement

Financial support for this work has been provided by the Office of Naval Research through contract number N0014-80-C-0345. Appreciation is expressed to Professor Ken Nobe for helpful discussion on nickel corrosion.

References

1. CRC Handbook of Chemistry and Physics, 1972.

2. Lange's Handbook of Chemistry, 11th edition.

3. Campbell, A. N., E. M. Kartzmark, and D. F. Williams, "The Conductance of Molten Lithium Chlorate and the Effect of Addition of Traces of Nonelectrolytes on the Conductance," Can. J. Chem. 40, 390 (1962).

4. Markowitz, M. M., D. A. Boryta, and H. Stewart Jr., "The Differential Thermal Analysis of Perchlorate VI. Transient Perchlorate Formation during the Pyrolysis of the Alkali Metal Chlorate," J. Phys. Chem. 68, 2282 (1964).

5. Markowitz, M. M., D. A. Boryta, and H. Stewart Jr., "Thermoanalytical Study of Lithium Chlorate," J. Chem. and Eng. Data, 9, 573 (1964).

6. Latimer, W. M., "Oxidation Potential," 2nd Edition, Prentice-Hall, Inc., New York, (1952).

7. Campbell, A. N. and J. E. Griffith, "The System Lithium Chlorate-Lithium Chloride-Water at Various Temperature," Can. J. Chem., 34, 1647 (1956).

8. Krauss, C. A. and W. M. Burgless, "A Study of the Properties of the System Lithium Chlorate-Water. I. Introduction. II Phase Relations." J. Am. Chem. Soc., 49, 1226 (1927).

9. Levich, V. G., "Physiochemical Hydrodynamics," Prentice-Hall, Inc., New Jersey, (1962).

10. Campbell, A. N. and M. K. Nagarajan, "Studies on the Thermodynamics and Conductances of Molten Salts and Their Mixture, Part II. The Viscosities, Heats of Fusion, and Heat Capacities of Lithium Chlorate-Lithium Nitrate Mixture," Can. J. Chem. 42, 1616 (1964).

11. Campbell, A. N. and M. K. Nagarajan, "Studies on the Thermodynamics and Conductances of Molten Salts and Their Mixtures, Part I. The Densities and Molar Volumes of Lithium Chlorate and of Lithium Chlorate-Lithium Nitrate Mixture," Can. J. Chem. 42, 1137 (1964).

12. Shen, D. H., "Lithium-Aluminum Alloy Electrodes in Lithium Chlorate," M.S. Thesis, Chemical Engineering Department, University of California, Los Angeles, 1979.


DATE
ILME